Journal of Colloid and Interface Science 468 (2016) 176–182

Contents lists available at ScienceDirect

Journal of Colloid and Interface Science

journal homepage: www.elsevier.com/locate/jcis

Oxygen functional groups in graphitic carbon nitride for enhanced photocatalysis

Shizhen Liu [a], Degang Li [a,b], Hongqi Sun [a,*], Ha Ming Ang [a], Moses O. Tadé [a], Shaobin Wang [a,*]

[a] Department of Chemical Engineering and CRC for Contamination Assessment and Remediation of the Environment (CRC CARE), Curtin University, GPO Box U1987, WA 6845, Australia
[b] School of Chemical Engineering, Shandong University of Technology, Zibo 255049, PR China

GRAPHICAL ABSTRACT

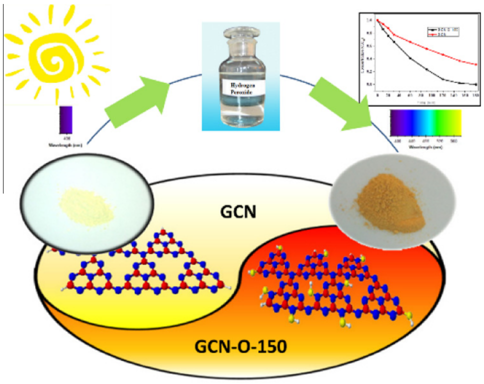

ARTICLE INFO

Article history:
Received 16 December 2015
Revised 20 January 2016
Accepted 23 January 2016
Available online 25 January 2016

Keywords:
Water treatment
Oxygen modification
Metal-free catalyst
Graphitic carbon nitride
Photodegradation

ABSTRACT

Metal-free semiconductors offer a new opportunity for environmental photocatalysis toward a potential breakthrough in high photo efficiency with complete prevention of metal leaching. In this study, graphitic carbon nitride (GCN) modified by oxygen functional groups was synthesized by a hydrothermal treatment of pristine GCN at different temperatures with H_2O_2. Insights into the emerging characteristics of the modified GCN in photocatalysis were obtained by determining the optical properties, band structure, electrochemical activity and pollutant degradation efficiency. It was found that the introduction of GCN with oxygen functional groups can enhance light absorption and accelerate electron transfer so as to improve the photocatalytic reaction efficiency. The photoinduced reactive radicals and the associated photodegradation were investigated by in situ electron paramagnetic resonance (EPR). The reactive radicals, $^{\cdot}O_2^-$ and $^{\cdot}OH$, were responsible for organic degradation.

1. Introduction

A modern society heavily depends on massive energy consumption, which inevitably results in energy crisis and environmental deterioration. Solar energy is a cheap, abundant and sustainable energy resource, and has been widely acknowledged as a fascinating alternative to fossil fuels. Solar cells [1], solar fuels [2], and environmental photocatalysis [3] have been extensively investigated for efficient solar energy utilization. Heterogeneous photocatalysis has attracted particular attention because of its great potential for environmental remediation using solar energy, simultaneously addressing both critical issues of energy shortage and environmental pollution [4–9]. The photocatalysis in practical applications is

---

* Corresponding authors.
E-mail addresses: h.sun@curtin.edu.au (H. Sun), Shaobin.wang@curtin.edu.au (S. Wang).

http://dx.doi.org/10.1016/j.jcis.2016.01.051

critically dependent on the photocatalytic performances of catalyst materials. Over the past four decades, numerous materials have been employed as photocatalysts, for example, metal oxides [4,8], metal sulfides [10], metal nitrides[11] and metal composites [12,13]. Among those semiconductor materials, TiO_2 is the most popular photocatalyst. However, the wide band gap energy (3.2 eV for anatase) and high recombination rate of the photoinduced carries have limited its practical applications [3,14,15]. Heteroatoms doping and other modification approaches have been used to manipulate the properties of TiO_2 photocatalysts [4,5,7,16,17], however, expected photocatalytic performance has not been yet achieved.

Recently, graphitic carbon nitride (GCN), a metal-free polymeric semiconductor, and its based composites are discerned to be promising photocatalysts for producing hydrogen by water splitting under visible light irradiations [18–20]. GCN molecular skeleton is based on tri-s-triazine (C_6N_7, also referred as melom) building blocks, which presents a layered structure as polycyclic aromatic hydrocarbons [21], and the electrons can transport between the dislocated π–π^* and n–π^* orbitals [22,23]. GCN also has an intrinsic band gap energy at 2.7 eV, which can be activated by visible light to produce electron/hole pairs [24]. Due to the high reduction ability originated from the high conduction band, GCN has demonstrated effective photoreduction for H_2 production and CO_2 reduction [18,19,25–30]. Recently, we applied different nanocarbons or polyoxometalate to modify GCN and enhanced photooxidation was obtained [31–33]. For a higher efficiency and wide applications, heteroatom doping using carbon, phosphorus, sulfur was also applied by other researchers to manipulate the properties of GCN [34–37].

In general, the doping technologies are able to manipulate multiple defects and distortion into a semiconductor system, leading to changes in electronic properties. The dopant heteroatom is required to have a diameter similar to or smaller than original atom, and the electronegativity of the dopant can be lower or higher than the target atom. As a result, the dopant could become a positive or negative centre in original cloud, then would restrain the electronic motivation [38]. The electronegativity of oxygen atom is 3.44 eV (in Pauling scale) and the atomic radius is 48 pm. The high electronegativity of oxygen could limit electronic mobility and protect photo-generated holes without lattice distortions. Therefore, oxygen was regarded as a good candidate for modification of GCN semiconductor. Li et al. [39] suggested that oxygen modification can enlarge surface area, improve physisorption and chemisorption, extend light absorption edge and then increase the photocatalytic activity [40–42]. Theoretical studies indicated that lower band gap energy can be obtained after oxygen modification of g-C_3N_4. The high concentration of oxygen alerts the direct semiconductor into an indirect semiconductor, meanwhile the negative oxygen atom becomes the active centre for enhanced light harvesting [42].

In this work, oxygen modification was achieved via a hydrothermal treatment of GCN with H_2O_2 solutions. Compared to the reported study [39], the effects of hydrothermal temperature on the characteristics such as crystalline structure, surface area, chemical states, optical property, band structure, recombination rate of carriers and photoelectrochemical properties were comprehensively investigated. The enhanced photocatalysis was confirmed by photodegradation of methylene blue and the related mechanism was studied by electrochemical analysis and electron paramagnetic resonance (EPR).

2. Experimental section

2.1. Chemicals and materials

Melamine, tert-butyl alcohol, 5,5-dimethyl-1-pyrroline N-oxide (DMPO) and p-benzoquinone (pBQ) in analytical grade were provided by Sigma–Aldrich. Hydrogen peroxide at 30 wt%, methylene blue, sulfuric acid, $K_3[Fe(CN)_6]$, KCl, Nafion, Na_2SO_4, NaOH, KH_4PO_4 were obtained from Biolab, Australia

2.1.1. Synthesis of graphitic carbon nitride

Graphitic carbon nitride was prepared by calcination of melamine powder [43]. Typically, 10 g melamine was dissolved in 10 mL methanol in a 20 mL alumina crucible. Then the crucible was put into an oven for drying at 60 °C for 24 h and then heated in a muffle furnace with a semi-closed cover. The sample was firstly heated at 400 °C for 2 h and then heated at 520 °C with a heating rate of 1 °C/min for another 2 h. The produced yellow particles were named as GCN.

2.1.2. Preparation of oxygen modified GCN

Typically, one gram GCN was placed in a 120 mL Teflon-lined stainless steel autoclave. Then 50 mL hydrogen peroxide solution was added and the mixed solution was kept stirring for 10 min. After that the autoclave was put into an oven for a hydrothermal treatment at four different temperatures (110, 130, 150, and 180 °C, respectively) for 12 h. The orange precipitate was collected by filtration and washed by 200 mL deionization water for three times. The final products, GCN-O-x (x is the hydrothermal temperature), were dried in a vacuum oven at 40 °C for 24 h.

2.2. Characterization of materials

X-ray diffraction (XRD) was used to observe the chemical phases of samples on a Bruker D8-Advance X-ray diffractometer. The chemical composition was determined using both the energy dispersive X-ray spectroscopy (EDS) and X-ray photoelectron spectroscopy (XPS) on a Thermo Escalab 250 with Al Kα X-ray, calibrated with the C 1s peak at 284.6 eV. Fourier transform infrared spectroscopy (FTIR) was performed on a Perkin–Elmer FTIR-100 with a MIR detector. Field emission scanning electron microscopy (FE-SEM) was used to analyze the morphology, size and textural information of the samples on Zeiss Neon 40EsB. UV–vis diffuse reflectance spectra (DRS) of samples were recorded on a JASCO V670 spectrophotometer with an Ø60 mm integrating sphere, and $BaSO_4$ as a reference material. Photoluminescence spectra were acquired on a spectrometer from Agilent technologies. Thermogravimetric-differential thermal analysis (TG-DTA) was carried out on a Mettler-Toledo instrument under an air flow at a heating rate of 10 °C/min. The Brunauer–Emmett–Teller (BET) surface area and the pore size distribution of the samples were evaluated by N_2 adsorption–desorption isotherm using a Micromeritics Tristar 3000. Prior to measurement, samples were degassed at 100 °C overnight under vacuum condition. Electron paramagnetic resonance (EPR) experiments were carried out on a Bruker EMX-E spectrometer (Germany). DMPO was applied as the radical capturing agent. EPR settings were centerfield at 3514.5 G; data collected within 100 G range; microwave frequency was 9.87 GHz; modulation frequency was 100 GHz; wattage is 18.11 mW.

2.3. Evaluation of photocatalytic performance

Photocatalytic performances of various catalysts were evaluated by the photodegradation of methylene blue (MB) under both artificial solar light and visible light irradiations. In a typical process, MB solutions (10 mg/L, 200 mL) and photocatalysts (100 mg) were mixed in a 1 L double-jacket cylindrical reactor with cooling water (25 °C) under constant stirring at 350 rpm. The photocatalytic reactor was positioned 30 cm below the light source. Two light sources were employed. One was UV–vis light with intensities at 2.31×10^{-3} mW/cm^2 (220–280 nm), 6.94 mW/cm^2 (315–400 nm),